

Supporting Information

Synthesis, crystal structures, two-photon absorption properties and application in biological imaging of A- π -D- π -A pyridinium salts

Zhaodi Liu,^{a,b} Fuying Hao,^a Huajie Xu,^a Hui Wang,^b Jieying Wu,^{*b} Yupeng Tian^{*b}

^a Department of chemistry and materials engineering, Fuyang Normal College, Fuyang, 230039, P. R. China.

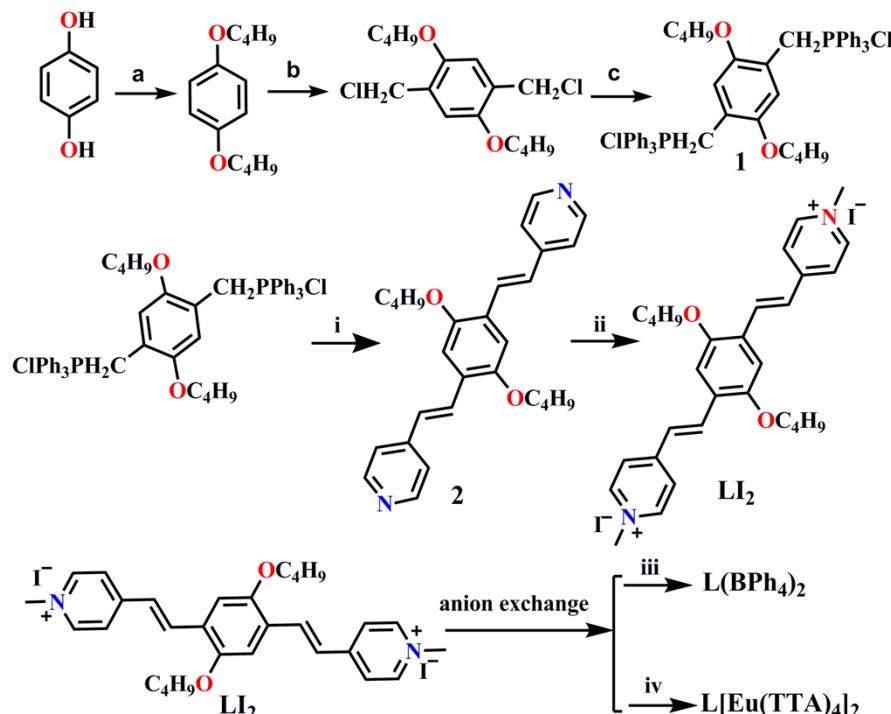
^b Department of Chemistry, Anhui Key Lab of Functional Inorganic Materials, Anhui University, 230039, Hefei, P. R. China.

*E-mail address: yptian@ahu.edu.cn. Tel: +86-5515108151. Fax: +86-5515107342.

1. Detailed experimental procedures
2. X-ray crystallography
3. Fluorescence lifetime measurement
4. Photophysical data of all the compounds
5. Figures

1. Detailed experimental procedures:

Synthetic route for LiI_2 , $\text{L}(\text{BPh}_4)_2$ and $\text{L}[\text{Eu}(\text{TTA})_4]_2$



1,4-dibutoxybenzene (1)

Hydroquinone (11.13 g, 0.10 mol) and sodium hydroxide (8.35 g, 0.21 mol) were dissolved in ethanol. 1-Bromobutane (27.97 g, 0.20 mol) was added dropwise to the solution and refluxed for 8 h. And then the solution was poured into water (1 L), the precipitate was filtered off and recrystallized from ethanol to give compound 1 as a white solid in 85% yield. ^1H NMR (400 MHz, d_6 -DMSO, δ) 6.624 (s, 4H, -ArH), 3.896~3.863 (m, 4H, - CH_2 -), 1.692~1.622 (m, 4H, - CH_2 -), 1.466~1.373 (m, 4H, - CH_2 -), 0.942~0.905 (m, 6H, - CH_3); IR (KBr, cm^{-1}), 2958, 1869, 1639, 1510, 1237, 1043, 831, 767, 535.

1,4-dibutoxy-2,5-bis(chloromethyl)benzene (2)

To a stirred solution of 1 (5.56 g, 0.025 mol), 20 mL dioxane and 50 mL concentrated hydrogen chloride was added three 50 mL portions of 40%

formalin at 20 min intervals. During the period of addition, hydrogen chloride gas was passed through. Stirring and the introduction of hydrogen chloride gas were continued for 3 h longer. And then 150 mL concentrated hydrogen chloride was added. After cooling, the formed solid materials was filtered off, and recrystallized by ethanol to give compound 2 as white crystals in 75% yield. ¹H NMR (400 MHz, d₆-DMSO, δ) 6.935 (s, 4H), 4.653 (s, 4H), 4.029~3.997 (m, 4H), 1.843~1.773 (m, 4H), 1.595~1.513 (m, 4H), 1.026~0.989 (m, 6H); IR (KBr, cm⁻¹) 2960, 1650, 1514, 1415, 1259, 1223, 1044, 867, 755, 608.

4-bis[(methyl)triphenylphosphonium chloride]-2,5-dibutoxybenzene (3)

A solution of compound 2 (5.23 g, 0.016 mol) and triphenylphosphine (8.92 g, 0.034 mol) in 100 mL of anhydrous ethanol was stirred and refluxed for 8 h. After distilling ethanol and washing with benzene three times, the white solid 3 was obtained in 93% yield. The product obtained was used in the next step without characterization.

Synthesis of 2,5-Dibutoxy-1,4-bis[2-(4-pyridyl)ethenyl]-benzene

To a solution of 4-bis[(methyl)triphenylphosphonium chloride]-2,5-dibutoxybenzene (8.45 g, 10 mmol), *t*-BuOK (4.49 g, 40 mmol) in *t*-BuOH (150 mL) was added 4-pyridinecarbaldehyde (2.35 g, 22 mmol) in *t*-BuOH (15 mL) and the solution was stirred overnight at room temperature. After removal of *t*-BuOH, the residue was diluted with DCM(100 mL) and washed with water, dried, and concentrated. The residue was purified by column chromatography (silica gel, ethyl acetate/hexane, 1:4) to give the title compound BPB as a yellow solid (3.13 g, 73%). ¹H NMR (400 MHz, DMSO-*d*₆) δ: 8.58 (d, *J* = 5.5 Hz, 4H), 7.66 (d, *J* = 16 Hz, 2H), 7.5 (d, *J* = 5.3 Hz, 4H), 7.39 (d, *J* = 16 Hz, 2H), 7.39 (s, 2H), 4.11(t, *J* = 6.3 Hz, 4H), 1.82 (m, 4H), 1.53 (m, 4H), 0.99(t, *J* = 7.3

Hz, 6H). ^{13}C NMR (100 MHz, CDCl_3) δ 151.33, 150.30, 145.06, 127.86, 126.65, 126.63, 120.99, 110.87, 69.03, 31.63, 19.46, 13.83; MALDI-TOF MS m/z in the positive mode: 429.254 (L+H).

Synthesis of pyridinium derivatives:

LI₂ To a solution of 2,5-Dibutoxy-1,4-bis[2-(4-pyridyl)ethenyl]-benzene (1.07g, 2.5 mmol) in dichloromethane (50 mL), iodomethane (1.41g, 10 mmol) in ethanol (100 mL) was added at room temperature for 1.5 h, then warmed to 80 °C to give a red solid in 74 % yield. ^1H NMR (400 MHz, $\text{DMSO}-d_6$) δ : 8.87 (d, J = 6.1 Hz, 4H), 8.22 (d, J = 6.1 Hz, 4H), 8.04 (d, J = 16.4 Hz, 2H), 7.72 (d, J = 16.4 Hz, 2H), 7.53 (s, 2H), 4.28 (s, 6H), 4.18 (t, J = 6.3 Hz, 4H), 2.11 – 1.70 (m, 4H), 1.67 – 1.38 (m, 4H), 1.00 (t, J = 7.3 Hz, 6H). FT-IR (KBr, cm^{-1}): 3424 (w), 3049 (w), 2932 (w), 1642 (m), 1613 (s), 1519 (m), 1496 (m), 1383 (s), 1208 (s), 1062 (w), 980 (w), 874 (w), 829 (w), 521 (w). MALDI-TOF MS m/z in the positive mode: 458.300 (L). Anal. Calcd for $\text{C}_{30}\text{H}_{38}\text{I}_2\text{N}_2\text{O}_2$: C, 50.32; H, 5.42; N, 3.41 %. Found: C, 50.58; H, 5.38; N, 3.93 %.

L(BPh₄)₂ To a solution of LI₂ (0.106 g, 0.15 mmol) in ethanol 50 mL, NaBPh₄ (0.1027 g, 0.3 mmol) in ethanol (10 mL) was added at room temperature for 0.5 h, then warmed to 80 °C to give a yellow solid 0.1420 g in 86.4 % yield. Then it was dissolved in DMF solution at room temperature. Black needle crystals were obtained for 20 days. ^1H NMR (400 MHz, $\text{DMSO}-d_6$) δ : ^1H NMR (400 MHz, $\text{DMSO}-d_6$) δ : 8.81 (d, J = 5.9 Hz, 4H), 8.16 (d, J = 5.9 Hz, 4H), 8.02 (d, J = 16.3 Hz, 2H), 7.66 (d, J = 16.5 Hz, 2H), 7.49 (s, 2H), 7.17 (s, 16H), 6.92 (t, J = 7.4 Hz, 16H), 6.78 (t, J = 7.2 Hz, 8H), 4.22 (d, J = 12.3 Hz, 6H), 4.15 (t, J = 6.3 Hz, 4H), 1.93 – 1.76 (m, 4H), 1.52 (dd, J = 14.5, 7.2 Hz,

4H), 0.99 (t, $J = 7.3$ Hz, 6H). FT-IR (KBr, cm^{-1}): 3451 (w), 3053 (m), 2960 (w), 1640 (m), 1613 (s), 1515 (m), 1477 (m), 1425 (m), 1396 (w), 1330 (w), 1194 (m), 1152 (w), 1032 (w), 972 (w), 867 (w), 846 (w), 739 (s), 708 (s), 610 (m). MALDI-TOF MS m/z in positive mode: 458.293 (L), in negative mode: 319.178 (BPh_4)⁻. Anal. Calcd for $\text{C}_{78}\text{H}_{78}\text{B}_2\text{N}_2\text{O}_2$: C, 85.23; H, 7.25; N, 2.46 %. Found: C, 85.39; H, 7.17; N, 2.55 %.

$\text{L}[\text{Eu}(\text{TTA})_4]_2$ To a mixture of triethylamine (0.131 g, 1.3 mmol) and HTTA (0.29 g, 1.3 mmol) in ethanol (10 mL), $\text{Eu}(\text{NO}_3)_3 \cdot 6\text{H}_2\text{O}$ (0.133 g, 0.3 mmol) in ethanol (10 mL) was added at room temperature for 30 min, then Li_2 (0.106 g, 0.15 mmol) in ethanol 20 mL was added, warmed to 80 °C giving a red solid 0.2 g in 52.7 % yield. Then it was dissolved in DMF solution at room temperature. Red block crystals were obtained for 30 days. ^1H NMR (400 MHz, $\text{DMSO}-d_6$) δ : 8.97 (d, $J = 5.8$ Hz, 4H), 8.24 (d, $J = 5.9$ Hz, 4H), 8.06 (d, $J = 16.4$ Hz, 2H), 7.71 (d, $J = 16.4$ Hz, 2H), 7.50 (d, $J = 18.7$ Hz, 12H), 7.02 (s, 1H), 6.88 – 6.14 (m, 14H), 5.59 (s, 1H), 4.36 (s, 6H), 4.17 (t, $J = 6.1$ Hz, 4H), 3.67 (s, 6H), 1.92 – 1.81 (m, 4H), 1.53 (dd, $J = 14.6, 7.3$ Hz, 4H), 1.00 (t, $J = 7.2$ Hz, 6H). FT-IR (KBr, cm^{-1}): 3450 (w), 1610 (s), 1538 (m), 1504 (w), 1471 (w), 1412 (m), 1357 (m), 1303 (m), 1247 (m), 1229 (m), 1183 (m), 1131 (m), 10061 (w), 968 (w), 931 (w), 861 (w). MALDI-TOF MS m/z in positive mode: 458.293 (L), in negative mode: 1036.879 $[\text{Eu}(\text{TTA})_4]^-$, 815.851 $[\text{Eu}(\text{TTA})_3]$. Anal. Calcd for $\text{C}_{94}\text{H}_{70}\text{Eu}_2\text{F}_{24}\text{N}_2\text{O}_{18}\text{S}_8$: C, 44.68; H, 2.83; N, 1.15 %. Found: C, 44.59; H, 2.79; N, 1.11 %.

2. X-ray crystallography

The crystal structures were determined by single crystal X-ray analyses. Data collections were performed using a Siemens SMART CCD area detector

diffractometer with Mo/K α radiation with an ω -scan mode [$\lambda = 0.71073$ Å]. The structures were solved with direct methods using the SHELXTL program [1] and refined anisotropically with SHELXTL using full-matrix least squares procedure. All non-hydrogen atoms were refined anisotropically. Crystallographic data, the selected bond lengths (Å) and Angles (°) of **L(BPh₄)₂**, **L[Eu(TTA)₄]₂** are presented in Table S1

Table S1. Selected Bond Lengths (Å) and Angles (°) for **L(BPh₄)₂**, **L[Eu(TTA)₄]₂**.

L(BPh₄)₂					
B(1)-C(16)	1.641(5)	B(1)-C(22)	1.644(5)	C(16)-B(1)-C(34)	102.6(3)
B(1)-C(34)	1.641(5)	B(1)-C(28)	1.644(5)	C(16)-B(1)-C(22)	112.1(3)
C(12)-O(1)	1.419(5)	C(22)-B(1)-C(28)	104.7(3)	C(34)-B(1)-C(22)	112.9(3)
C(1)-N(1)	1.480(5)	C(8)-C(7)-C(4)	126.7(4)	C(16)-B(1)-C(28)	112.8(3)
C(7)-C(8)	1.316(5)	O(1)-C(10)-C(9)	115.4(3)	C(34)-B(1)-C(28)	112.0(3)
C(8)-C(9)	1.461(5)	O(1)-C(10)-C(11)	124.1(3)	C(2)-N(1)-C(1)	119.6(3)
C(4)-C(7)	1.451(5)	C(8)-C(7)-C(4)	126.7(4)	C(7)-C(8)-C(9)	125.2(4)
L[Eu(TTA)₄]₂					
C(1)-N(1)	1.486(9)	C(27)-S(2)	1.674(8)	C(16)-S(1)	1.646(9)
C(7)-C(8)	1.299(10)	C(35)-S(3)	1.688(10)	C(19)-S(1)	1.712(6)
C(8)-C(9)	1.463(9)	C(32)-S(3)	1.634(10)	C(24)-S(2)	1.640(12)
C(4)-C(7)	1.456(9)	C(40)-S(4)	1.650(13)	Eu(01)-O(6)	2.395(5)
C(12)-O(1)	1.412(10)	C(43)-S(4)	1.636(10)	Eu(01)-O(5)	2.401(4)
Eu(01)-O(2)	2.392(4)	Eu(01)-O(7)	2.373(4)	Eu(01)-O(9)	2.431(5)
Eu(01)-O(4)	2.395(4)	Eu(01)-O(8)	2.382(5)	Eu(01)-O(3)	2.391(4)
O(7)-Eu(01)-O(8)	85.23(17)	O(3)-Eu(01)-O(6)	122.06(17)	O(8)-Eu(01)-O(5)	137.17(17)
O(7)-Eu(01)-O(3)	78.60(15)	O(2)-Eu(01)-O(6)	149.47(17)	O(3)-Eu(01)-O(5)	71.81(15)
O(8)-Eu(01)-O(3)	150.81(17)	O(7)-Eu(01)-O(4)	143.86(16)	O(2)-Eu(01)-O(5)	87.73(16)
O(7)-Eu(01)-O(2)	139.67(16)	O(8)-Eu(01)-O(4)	72.43(16)	O(6)-Eu(01)-O(5)	74.87(18)
O(8)-Eu(01)-O(2)	105.64(16)	O(3)-Eu(01)-O(4)	132.54(15)	O(4)-Eu(01)-O(5)	72.21(15)
O(3)-Eu(01)-O(2)	73.58(14)	O(2)-Eu(01)-O(4)	75.08(15)	O(7)-Eu(01)-O(9)	73.37(18)

O(7)-Eu(01)-O(6)	70.77(18)	O(6)-Eu(01)-O(4)	75.78(17)	O(8)-Eu(01)-O(9)	69.88(17)
O(8)-Eu(01)-O(6)	73.66(18)	O(7)-Eu(01)-O(5)	110.70(18)	O(3)-Eu(01)-O(9)	82.20(16)
O(2)-Eu(01)-O(9)	74.40(16)	O(6)-Eu(01)-O(9)	130.13(17)	O(4)-Eu(01)-O(9)	121.78(17)
O(5)-Eu(01)-O(9)	151.84(16)	C(2)-N(1)-C(1)	119.8(6)	C(8)-C(7)-C(4)	125.3(7)
C(7)-C(8)-C(9)	127.0(7)	C(32)-S(3)-C(35)	91.1(6)	C(24)-S(2)-C(27)	93.6(6)
C(43)-S(4)-C(40)	93.1(7)	C(16)-S(1)-C(19)	91.9(4)	O(1)-C(11)-C(10)	125.3(7)

3. Fluorescence lifetime measurement:

The fluorescence lifetime was measured using the time-correlated single-photon-counting (TCSPC) technique (Horiba) with excitation source NanoLed® 375 nm impulse repetition rate 1 MHz (Horiba) at 90 °C to the R928P detector (Hamamatsu Photonics, Japan). The detector was set to 453 nm with a 10 nm bandpass. The electrical signal was amplified by TB-02 pulse amplifier (Horiba) and the amplified signal was fed to the constant fraction discriminator CFD (Philips, The Netherlands). The first detected photon was used as a Start signal by time-to-amplitude converter (TAC), the excitation pulse triggered the Stop signal. The multichannel analyzer (MCA) recorded repetitive start–stop signals from the TAC and generated a histogram of photons as a function of time-calibrated channels (6.88 ps / channel) until the peak signal reached 10000 counts. The lifetime was recorded on a 50 ns scale. The instrument response function was obtained using Rayleigh scatter of SiO₂ nanocrystals in H₂O sample in a quartz cuvette at 377 nm emission. The measurements were conducted at room. DAS6 v6.1 decay analysis software (Horiba) was used for lifetime calculations. The goodness of fit was judged by chi-squared values ($\chi^2 \approx 1$) (Table S2), Durbin–Watson parameters and visual observations of fitted line, residuals and autocorrelation function. One exponential decay equations were used for data fitting

4. Photophysical data of all the compounds

Table S2 Photophysical data of all the compounds.

Compound	$\lambda_{\text{ex}}^{\text{a}}$	$\lambda_{\text{em}}^{\text{b}}$	Φ^{c}	τ^{d}	σ^{e}
Ll_2	368, 465	580	0.219	3.77 (465 nm)	308
$\text{L}(\text{BPh}_4)_2$	368, 465	580	0.236	3.74 (465 nm)	111
$\text{L}[\text{Eu}(\text{TTA})_4]_2$	340, 465	615, 580	0.108, 0.216	3.72 (465 nm)	552

a Linear absorption maxima(nm). b Peak position of SPEF, excited at the absorption maximum. c Quantum yields measured using Rhodamine 6G as a standard. d Fluorescence lifetime (ns). e 2PA cross-section (GM, 1 GM = $10^{-50} \text{ cm}^4 \text{ s} \cdot \text{photon}^{-1}$).

5. Figures

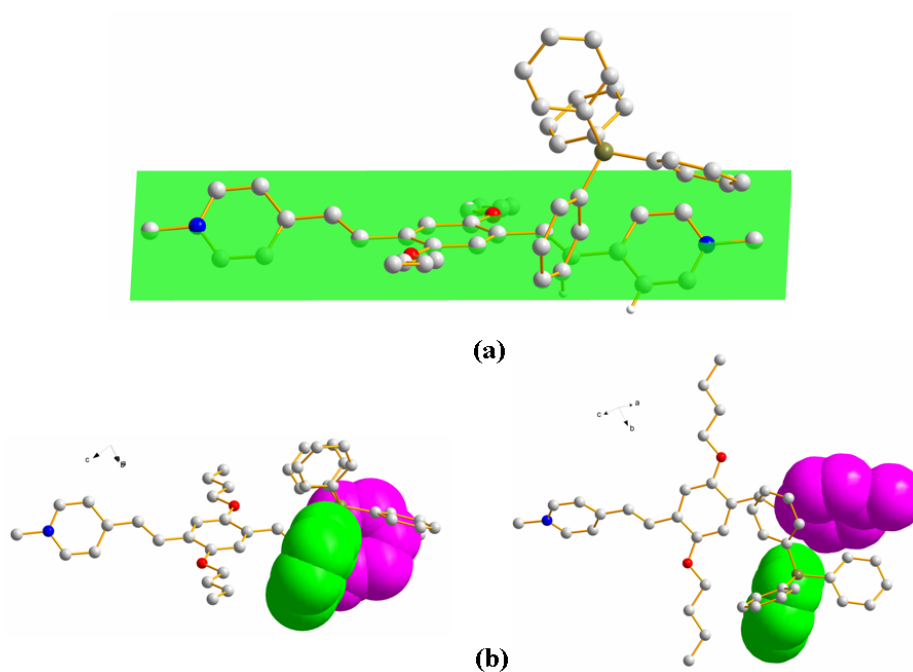


Fig. S1. The molecular diagram of $\text{L}(\text{BPh}_4)_2$, the close contact making the pyridine rings of L^{2+} twist with $50.1(4)^\circ$ from the benzene plane of L^{2+} (a), space filling for the pyridine rings of L^{2+} and the benzene plane of L^{2+} , highlighting the close contact (b).

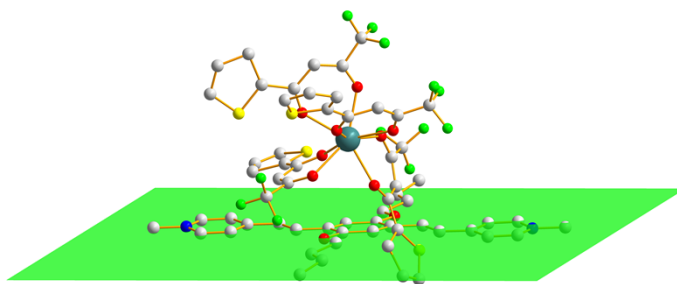


Fig. S2. The molecular diagram of $L[Eu(TTA)_4]_2$, showing no close contact for the anions and cation.

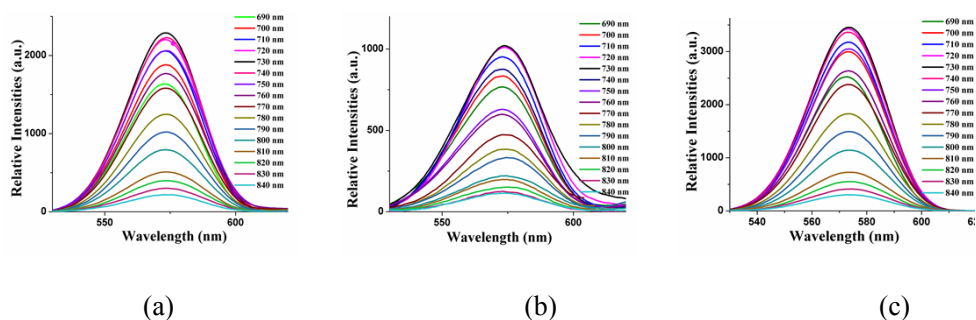


Fig. S3 TPEF of LI_2 (a), $L(BPh_4)_2$ (b) and $L[Eu(TTA)_4]_2$ (c) under different excitation wavelengths.

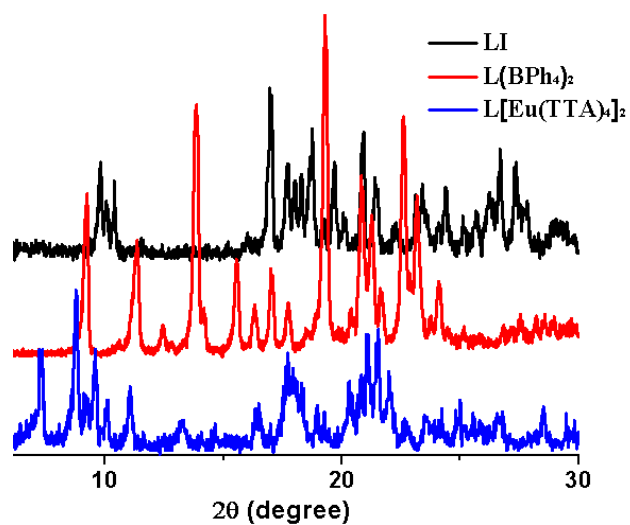


Fig. S4 As-experimental XRD patterns for LI_2 , $L(BPh_4)_2$ and $L[Eu(TTA)_4]_2$.

References:

[1] G. M. Sheldrick. Acta. Cryst. A. 2008.64, 112..